

# Formation and Spreading of Lipid Bilayers on Planar Glass Supports

Paul S. Cremer and Steven G. Boxer\*

Department of Chemistry, Stanford University, Stanford, California 94305-5080

Received: October 7, 1998; In Final Form: January 8, 1999

The fusion and spreading of phospholipid bilayers on glass surfaces was investigated as a function of pH and ionic strength. Membrane fusion to the support was favorable at high ionic strength and low pH for vesicles containing a net negative charge; however, neutral and positively charged vesicles fused under all conditions attempted. This result suggests that van der Waals and electrostatic interactions govern the fusion process. Membrane spreading over a planar surface was favorable at low pH regardless of the net charge on the bilayer, and the process is driven by van der Waals forces. On the other hand membrane propagation is impeded at high pH or on highly curved surfaces. In this case a combination of hydration and bending interactions is primarily responsible for arresting the spreading process. These results provide a framework for understanding many of the factors that influence the effectiveness of scratches on planar supported bilayers as barriers to lateral diffusion and lead to a simple method to heal these scratches.

## Introduction

Phospholipid vesicles self-assemble into fluid planar bilayers on solid supports<sup>1–3</sup> (Figure 1). A substantial body of evidence suggests that a thin water layer approximately 1–2 nm thick is trapped between the support and the headgroups of the lower leaflet of the bilayer.<sup>4–7</sup> This water layer acts as a lubricant allowing both leaflets of the bilayer to remain fluid. As a consequence, planar supported membranes retain many of the properties of free vesicles or even cell membranes when the appropriate surface components are present, and they are convenient to study with an array of surface-sensitive techniques.

The interactions between planar bilayers and oxide supports are controlled by van der Waals, electrostatic, hydration, and steric forces.<sup>8</sup> A subtle balance among these determines the kinetics of vesicle adsorption and fusion to the underlying support as well as membrane spreading across the surface. There have been only a few studies of the specific factors that govern bilayer–surface interactions.<sup>9–11</sup> More extensive investigations have been performed on the related subjects of supported bilayer–supported bilayer, surfactant–surface, and silica–silica interactions.<sup>12–16</sup>

We have found that it is possible to partition fluid-supported membranes into corralled regions that retain their fluidity using simple mechanical scratches.<sup>17,18</sup> One would expect, however, that supported membranes would spread into and heal the scratched region, similar to the process of membrane fusion that must occur on the surface to form a continuous supported membrane in the first place. This did not occur under the conditions we were investigating so the partitioning was essentially permanent. These partitioned surfaces have proven to be a useful experimental system for studying the properties of lipid bilayers<sup>19,20</sup> and as a new technology for studying cellular interactions with synthetic surfaces.<sup>21</sup> The purpose of the work presented here is to better understand the factors that affect the formation of supported membranes by vesicle fusion and the properties of mechanical scratches that lead to the partitioning. We demonstrate that the fusion of phospholipid vesicles to glass substrates is governed by the pH of the buffer and ionic strength in a manner that is correlated with the charge

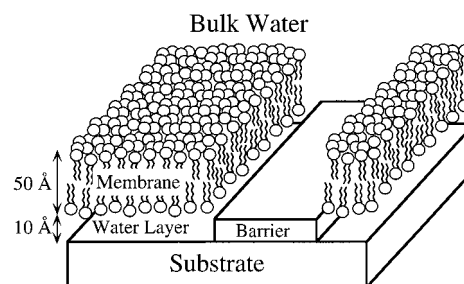


**Figure 1.** Schematic diagram of a planar supported lipid bilayer. A thin water layer approximately 1–2 nm thick is present between the lower leaflet of the bilayer and the oxide support.

on the membrane and on the support. This can be understood in terms of an attractive van der Waals interaction that is either enhanced or opposed by an additional electrostatic contribution that depends on conditions. The spreading process is driven by the same van der Waals forces that induce fusion. However, the spreading process can be inhibited by surface topography in combination with the pH of the aqueous solution above the exposed interface.

## Experimental Section

Small unilamellar vesicles (SUVs) composed of egg phosphatidylcholine (Avanti Polar lipid Inc., Alabaster, AL) mixed with low concentrations of fluorescent probe molecules were used to form supported lipid bilayers except where noted. The probes include *N*-(Texas Red sulfonyl)-1,2-dihexadecanoyl-*sn*-glycero-3-phosphoethanolamine, triethylammonium salt (Texas Red DHPE); 2,2-(*N*-(7-nitrobenz-2-oxa-1,3-diazol-4-yl)amino)-23,24-bisnor-5-cholesterol-3 $\beta$ -ol (NBD cholesterol); and 4-(4-(didecylamino)styryl)-*N*-methylpyridinium iodide (D291) (all from Molecular Probes, Eugene, OR). The charges on the probes [Texas Red DHPE (negative), NBD cholesterol (neutral), and D291 (positive)] were confirmed throughout the pH range (2.5–12.3) studied in these experiments by electrophoresis in the supported membrane as described previously.<sup>18</sup>

Supported planar lipid bilayers were prepared by vesicle fusion to glass surfaces.<sup>22</sup> Lipids were mixed with the appropri-

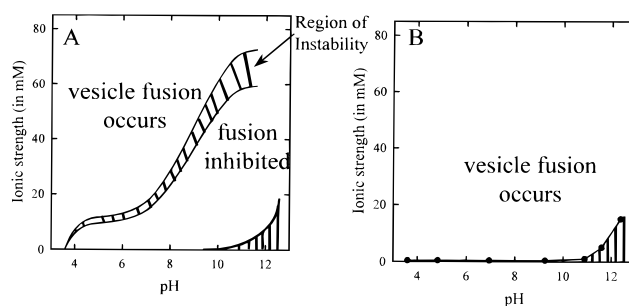
ate fluorescent probes in chloroform and dried under Ar followed by desiccation under house vacuum for at least 2 h. The mixtures were reconstituted in sodium phosphate solutions over the pH range of 2.5–12.3. Suspension of the lipids in solution was achieved by vortexing for several minutes at low speed. SUVs were formed by probe sonication to clarity of the suspended lipids over an ice water bath.<sup>23</sup> The solutions were centrifuged at 33 000 rpm for 30 min to remove titanium particles introduced during the sonication process. The supernatant was then centrifuged again at 45 000 rpm to separate larger lipid structures from the SUVs, which continued to remain in the supernatant. SUV solutions were stored at 4 °C until use.

Supported planar lipid bilayers were assembled by placing a glass coverslip (Baxter Scientific Products, McGaw, Park, IL) over a 60  $\mu$ L drop of SUV solution on the bottom of a crystallization dish. The coverslips were prepared by washing in ICN $\times$ 7 detergent (ICN, Costa Mesa, CA) followed by exhaustive rinsing in distilled water and then baking in a kiln at 425 °C for 4 h. Excess vesicles were washed away from the newly formed supported bilayers by shaking gently for approximately 20 s in buffer solution. This method yielded uniform membrane-covered surfaces where the phospholipid bilayer was in the fluid state as demonstrated by fluorescence recovery after photobleaching (FRAP, spot photobleaching) experiments. All experiments were conducted at 22 °C.

Fluorescent imaging of the samples was performed by still photography using a Nikon Labophot fluorescent microscope equipped with a 35 mm Nikon camera. Atomic force microscopy images of the substrates were obtained using a MultiMode Nanoscope SPM (Model MMAFM-2, Digital Instruments, Santa Barbara, CA). Cantilevers with oxide-sharpened silicon nitride tips from BioForce were utilized in tapping mode with a type J scanner.

## Results

**Vesicle Fusion to Glass Supports as a Function of Ionic Strength and pH.** When SUVs (1 mg/mL) prepared from egg PC and 1 mol % of Texas Red DHPE are brought into contact with a glass support from a pH 8 sodium phosphate buffer with an ionic strength of 75 mM, supported membranes are formed rapidly (less than 5 s). FRAP measurements demonstrate that they are fully fluid. By contrast, when identical lipid vesicles in a pH 11.6 sodium phosphate buffer solution at an ionic strength of 20 mM were used, little bilayer material adsorbed to the glass coverslip. This was true even if the vesicle solution was left in contact with the oxide surface for 24 h. The influence of the buffer on the fusion process was investigated systematically as a function of pH and ionic strength of the sodium phosphate buffer solution, and Figure 2A summarizes the results of many measurements. Fusion occurs at lower pH and higher ionic strength, whereas it is inhibited at higher pH and lower ionic strength. The narrow regime between these two conditions represents a region of instability. Under these conditions, the formation of supported lipid bilayers was uneven and not continuous over the entire slide. FRAP measurements showed further that fluidity was not completely or evenly achieved. The precise position of this boundary depends on the conditions under which the experiments were run. For example, adding even 1 ppm  $\text{Ca}^{2+}$  ions to the solution significantly shifted the fusion regime to higher pH and lower ionic strength; hence Tris, HEPES, and other buffers that contain trace concentrations of  $\text{Mg}^{2+}$  and/or  $\text{Ca}^{2+}$  ions were intentionally avoided. Further, switching brands of glass or changing the preparation method of the glass coverslips was also avoided as each affects the



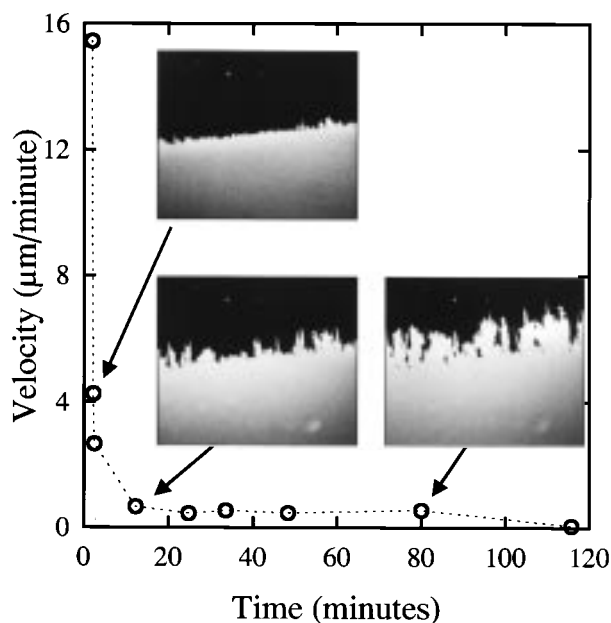
**Figure 2.** Phase diagrams of the fusion of small unilamellar vesicles to glass surfaces for egg phosphatidylcholine containing: (A) 1 mol % of the negatively charged fluorophore Texas Red DHPE; (B) 1 mol % of the positively charged fluorophore D291. The crosshatched areas in the center are regions of phase instability. The regions with vertical stripes in the lower right-hand corner of both diagrams serve to block out conditions where buffer formation is not possible.

diagram. Bilayer adhesion to the surface was apparently difficult to reverse, as raising the pH (or lowering the ionic strength) after a supported bilayer was formed would not remove the bilayer from the surface under the conditions of these experiments.

Fusion of egg PC vesicles containing 1 mol % of the positively charged D-291 probe was monitored in parallel experiments. As shown in Figure 2B, it was found that vesicle fusion took place at all pH and ionic strength values attempted. The slight rise in the curve at high pH merely reflects the ionic strength necessary to create buffered solutions at the corresponding pH values. Fusion of vesicles containing the neutral NBD-cholesterol probe showed the same behavior as that seen for the D-291, i.e., fusion occurred at all pH and ionic strength values attempted.

**Bilayer Spreading.** Fluid lipid bilayers can be easily removed from glass supports by drawing them through the air/water interface. In the experiments described in this section, bilayer-coated coverslips were partially drawn through the interface. The lipids remained where the support was still in contact with the aqueous solution, while the air-exposed portion of the surface became lipid free as the lipid material associated with it was peeled off and disperses in solution. The sample was then returned to the pH 8.0, 50 mM sodium phosphate buffer. At this point the supported lipid bilayer quickly began to creep over the bare portion of the planar glass support. The initial advance rate was greater than 15  $\mu\text{m}/\text{min}$ . As the bilayer expanded, the front speed slowed and continued to advance through fingerlike projections as previously observed by Rädler et al.<sup>10</sup> as the rate fell below 1  $\mu\text{m}/\text{min}$  (Figure 3). The three inset pictures with arrows correspond to points along the velocity vs time curve and show the increasing roughness of the bilayer edge during the expansion process. The “bilayer front” becomes ill defined as the roughening progressed. The front was therefore defined to be at the center of a narrow strip drawn perpendicular to the direction of motion that was 50% covered with the advancing bilayer. The bilayer was finally arrested after expansion to approximately 106% of its original size; this value is independent of the membrane’s initial area. Alternatively, when the sample is returned to a pH 11.6 buffer, the bilayer does not spread out at all and the bilayer edge remains straight.

Further experiments were performed by varying the pH and ionic strength values of the reimmersion buffer over a wide range to determine the conditions for which bilayer spreading is favorable (Figure 4). For these experiments, the bilayers were formed in a pH 8.0, 50 mM sodium phosphate buffer and then transferred to the solution of interest for the spreading experi-



**Figure 3.** The rate of spreading for an egg phosphatidylcholine membrane containing 1 mol % of the negatively charged fluorophore Texas Red DHPE on a borosilicate support in a 50 mM, pH 8.0 sodium phosphate buffer. Part of the slide supporting the membrane was exposed to air, removing the lipid layer. Spreading commenced from the unexposed region into the exposed region immediately upon returning the slide into the buffer solution. The inset pictures show snapshots of the spreading bilayer at various times. As the bilayer spreads over the surface the advancing profile becomes increasingly rough.

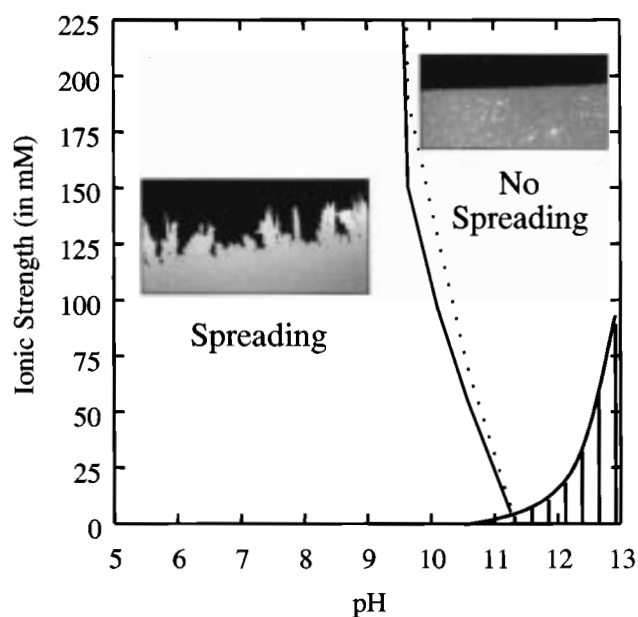


**Figure 4.** pH vs. ionic strength diagram of the spreading behavior of an egg phosphatidylcholine bilayer on borosilicate using the method illustrated in Figure 3: The solid line (—) represents 1 mol % negatively charged Texas Red while the dashed line (---) is for 1 mol % positively charged D-291. The two inset figures are typical images of the membrane front for a spreading and nonspreading bilayer 60 min after returning the system to buffer solution.

ment. As the pH of the re-immersion solution was raised, the initial rate of bilayer spreading became progressively slower. The solid line in the figure denotes the point at which the spreading rate of an egg PC bilayer containing 1 mol % Texas Red slowed to less than  $0.01 \mu\text{m}/\text{min}$ , at which point the rate

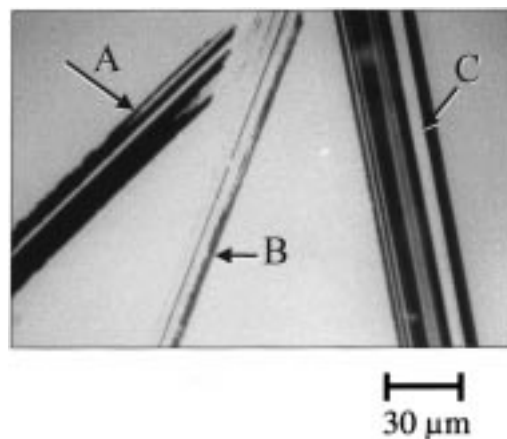


**Figure 5.** Epifluorescence image of a supported lipid bilayer formed in a 50 mM pH 8.0 sodium phosphate buffer, which has been mechanically scratched in three places (arrows A, B, and C) and then placed in a 50 mM pH 5.5 sodium phosphate buffer solution. The bilayer is beginning to expand back into the mechanically etched region healing over the scratch.

became difficult to measure. The dashed line in the figure represents a similar set of experiments performed with 1 mol % D-291, a positively charged fluorophore, in place of the Texas Red. Little difference was seen between the two curves.

#### Bilayer Spreading at Mechanically Modified Interfaces.

As noted in the Introduction, when the supported bilayer is scratched with a pair of tweezers or other sharp object at pH 8, a boundary to lateral diffusion is created that persists over an extended period of time.<sup>18,17</sup> Bilayer material is removed and the surface is abraded (see below). If the pH is lowered to 6.0 or below at an ionic strength of 50 mM, the bilayer spreads onto the modified portion of the surface to heal the scratched areas. High-magnification images of scratched regions during the healing process at low pH reveal that bilayer material creeps along the direction of the scratch in long lines (Figure 5). The region shown in the figure contains three scratch marks which have undergone various degrees of healing (A, healing just begun; B, nearly fully healed; C, an intermediate case). The process of healing typically takes place over several hours.

To test the effect of etch marks on bilayer spreading, lipid bilayers were formed on surfaces that had been mechanically scratched before vesicle adsorption. They were then partially drawn through the air/water interface and re-immersed in a pH 8.0 buffer solution as described in the last section (Figure 6a). The figure shows a scratch mark, which in part proceeds along the boundary between the lipid-covered and bare portion of the surface. After 30 min the egg PC bilayer with 1 mol % Texas Red DHPE has expanded over those portions of the surface that do not contain the scratch mark, while the scored part acts as a barrier to bilayer expansion (Figure 6b).

Two additional scratch lines can be seen in Figure 6 with their positions denoted by arrows on the right-hand side. These scratched regions appear lighter in the figure because lipid material remains adhered to them even after the coverslip is exposed to air. FRAP experiments on these regions demonstrate that the material is not assembled into a fluid lipid bilayer. It can be seen in Figure 6b that when the expanding bilayer reaches the scratch mark it becomes arrested (circled area).

Under the above conditions the spreading process could be induced over the scratched region by lowering the bulk pH to 6.0 or below; however, bilayer spreading at scratched regions was quite sensitive to the chemical content of the membrane. For example, further experiments with bilayers containing



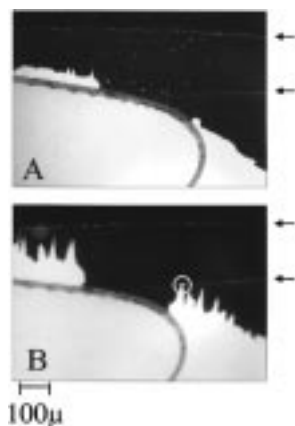


**Figure 6.** Time-elased epifluorescence images of a supported lipid bilayer expanding on an etched surface in a 50 mM, pH 8.0 sodium phosphate buffer. The upper image (A) was taken immediately after the system was formed, while the lower image (B) was taken 25 min later. The arrows point to two additional scratches. The bilayer is seen to expand on the smooth glass surface, but does not expand over the scratched region and is arrested as it approaches a scratch (circled feature).

mixtures of 30% cholesterol in egg PC showed little propensity for healing even when the bulk pH was lowered to 4.5. On the other hand, in studies with 10% phosphatidylserine in egg PC bilayers, the spreading proceeded over scratch marks up to pH 9.

AFM images of mechanically modified surfaces reveal that etch marks made in the underlying surface are 10–30 nm deep and approximately 10–30  $\mu\text{m}$  wide (Figure 7). It is also evident that their topography resembles the epifluorescence images of bilayer material spreading on scratched surfaces (Figure 5). A line profile across the scratch mark demonstrates that the surface gradient is quite steep even on the nanometer scale (Figure 7). For the sharpest scratch marks the surface altitude was seen to rise (or fall) as much as 7 nm over a 40 nm distance, corresponding to a rise/run ratio of 0.18.

## Discussion

**Fusion and Removal of Bilayer Material on Glass Supports.** The process of phospholipid vesicle fusion with unroughened glass supports seems to be governed by the same Derjaguin–Landau–Verwey–Overbeek (DLVO) forces that are responsible for colloid aggregation and deposition.<sup>8</sup> DLVO theory models the forces in such systems as consisting of an electrostatic interaction acting in combination with a van der Waals attraction, where the electrostatic portion is calculated from the Poisson–Boltzmann equation. In the present experiments only the glass surface has titratable OH groups, while the charge density on the surface of the lipids remains fixed over the range of pH values used. Under conditions of low pH and high ionic strength, negatively charged vesicles readily adsorb and fuse to the surface due to the favorable van der Waals forces (Figure 2a). As the pH of the buffer is raised (or the ionic strength is lowered), the electrostatic repulsion between the surface and negatively charged vesicles increases and eventually overwhelms the van der Waals attraction. In this case the surface remains virtually lipid free. However, under conditions where the two forces are nearly in balance there is not a sharp transition between conditions where vesicle adhesion and fusion occurs and where it is prevented. Instead, a narrow region of instability exists where vesicle fusion occurs in some areas, but not in others. This is probably related to lateral heteroge-

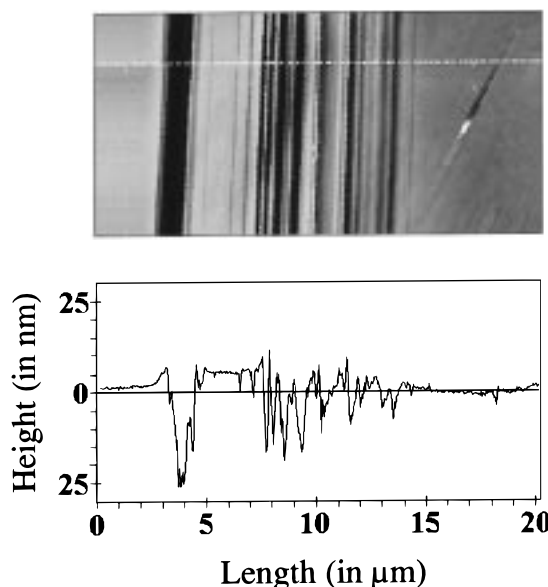


**Figure 7.** Atomic force micrograph and line profile of a glass substrate which has been scratched by tweezers in the vertical direction. The dust spot on the right side of the image indicates the scanning direction of the silicon nitride tip. The scratch mark is about 12  $\mu\text{m}$  in width and tens of nanometers deep.

neities in the roughness and chemical composition of the float glass cover slips used for these experiments.

The general shape of the phase boundary between fusion and nonfusion conditions for negatively charged vesicles shows a good deal of structure (Figure 2a). At pH 4 there is a small shoulder followed by a broader rise centered around pH 9. These features correspond roughly with the known  $\text{pK}_a$  values for silica surfaces.<sup>24</sup> This is consistent with the notion that the variation in charge density as a function of pH for the glass coverslips employed in our experiments is similar to that of pure silica. This is perhaps surprising as multicomponent glass surfaces might be expected to exhibit more complex behavior owing, for example, to the presence of surface boranol groups in addition to the silanol groups that would be found on  $\text{SiO}_2$ . Previous results from borosilicate gels have shown that surface silanol groups are somewhat less acidic on multicomponent surfaces than on simple silica surfaces.<sup>25</sup> However, boranol groups in these systems are somewhat more acidic than the silanol groups, and these two effects may function to cancel one another leaving the glass surfaces with similar properties to pure silica. In any event the features in Figure 2a are quite broad and may be masking a larger heterogeneity of  $\text{pK}_a$  values.

It is difficult to quantitatively calculate the position and shape of the vesicle fusion/nonfusion boundary in Figure 2a from simple DLVO theory as the interfacial water thickness and surface charge density are not well characterized for multicomponent glass systems. Furthermore, recent work suggests that at short distances a repulsive force due to either steric or hydration forces may dominate both the van der Waals and electrostatic forces, limiting the utility of DLVO theory at short range.<sup>26,27</sup> However, a simple calculation confirms that a model consisting only of van der Waals and electrostatic forces is at least of some use in the present case. If we assume that there are approximately four titratable OH groups/ $\text{nm}^2$  on the glass surface (a value similar to that found for silica<sup>25</sup>) then the maximum value for the surface charge density,  $\sigma_{\text{max}}$ , is 0.64 C/ $\text{m}^2$ . Figure 2a shows that above pH 10.5 the ionic strength of the buffer solution required for vesicle fusion to occur levels off near a value of 65 mM. If we interpret this occurrence as

the approach to full surface deprotonation, then the charge density at the surface should be close to  $\sigma_{\max}$  above this pH. At  $\sigma_{\max}$  and an ionic strength of 65 mM the surface potential,  $\Psi_s$ , is approximately 67 mV and the potential at the lower leaflet of the bilayer,  $\Psi_b$ , is 6.7 mV ( $\sigma_b = 0.01 \text{ C/m}^2$ ) according to the Grahame equation for a 1:1 electrolyte solution:

$$\sigma_i = \sqrt{8\epsilon\epsilon_0 kT [\text{Na}^+]} \sinh(e\Psi_i/2kT)$$

For two planar surfaces with different charge densities the electrostatic repulsion energy,  $W$ , is

$$W = (64kT[\text{Na}^+]\tanh(e\Psi_s/4kT)\tanh(e\Psi_b/4kT)/\kappa)e^{-\kappa D}$$

where  $\kappa$  is the Debye length and  $D$  is the distance between the lower leaflet of the bilayer and the support surface. Inserting the estimated values for the surface potentials one obtains a repulsive interaction of approximately  $2 \times 10^{-4} \text{ J/m}^2$  between the lower leaflet of the bilayer and the glass surface. The van der Waals interaction energy for two planar surfaces is

$$W(D) = -A/12\pi D^2$$

where  $A$  is the Hamaker constant. Assuming a van der Waals attraction energy that just balances the electrostatic repulsion and using Rädler et al.'s value for the Hamaker Constant between phospholipids and silica of  $4 \times 10^{-21} \text{ J}$ ,<sup>10</sup> we obtain a distance of 1 nm between the glass surface and the lower leaflet of the bilayer. This value is in good agreement with previous measurements of the water layer thickness.<sup>4-7</sup>

**Spreading of Phospholipid Bilayers on Smooth versus Mechanically Roughened Surfaces.** The spreading of lipid bilayers on smooth surfaces proceeds at low pH regardless of the ionic strength of the buffer or the net charge on the membrane (Figure 4). The driving force for this process is almost certainly the same attractive van der Waals interaction that promotes vesicle fusion. At high pH the spreading process is inhibited for both negatively and positively charged membranes and is nearly independent of the ionic strength of the buffer. This is a clear indication that electrostatic forces are not directly responsible for arresting the membrane spreading process. Indeed, it would be expected that a purely electrostatic interaction would be attenuated as the ionic strength of the buffer is raised, an effect that is not observed. Instead, we suggest that spreading is prevented by changes in the hydration of the surface under basic conditions. Previous studies using nonlinear optical techniques have demonstrated that water molecules at the silica/buffer interface become ordered as the pH is raised.<sup>24,28</sup> Infrared-visible sum frequency generation experiments by Du et al. have shown that the vibrational spectra of near surface water molecules at pH 12 correspond closely to that of an ice-like layer. Such a layer would be a poor lubricant for the expanding bilayer if the spreading process requires the facile realignment of water molecules as the membrane front advances.

At low pH the initial spreading process is quite rapid, but slows down over the course of a few minutes and stops completely after about 6% expansion of the membrane (Figure 3). Previous bilayer spreading studies by Rädler et al. have shown that the spreading rate of phospholipid material from a lipid reservoir decelerates with time as  $t^{-0.5}$ .<sup>10</sup> The authors attributed the deceleration rate to frictional interactions between the bilayer and the surface as bilayer material continuously proceeds outward from the lipid reservoir. In the present experiments the rate of deceleration is even faster as no source of excess lipid material is available for the spreading process

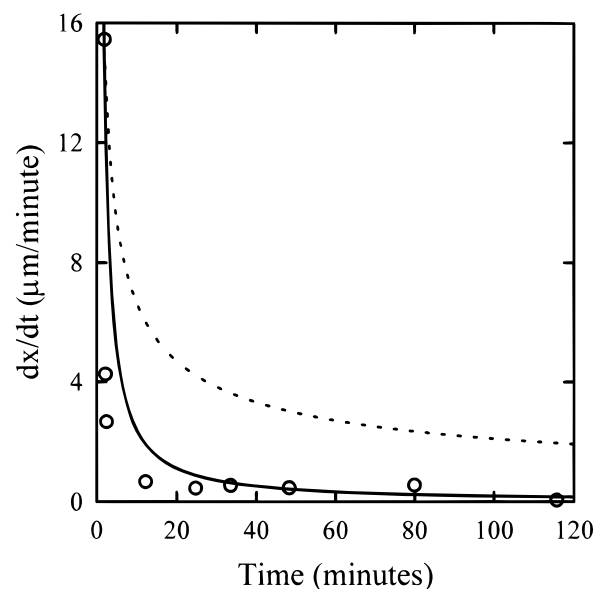


**Figure 8.** Fitting curves for the spreading rate of a lipid bilayer frontier with time on a smooth glass surface under conditions described in Figure 3. The circles (O) represent the measured data points, while the solid line (—) is a  $1/t^{1/2}$  fit and the dashed line (---) is a  $1/t$  fit to the data.

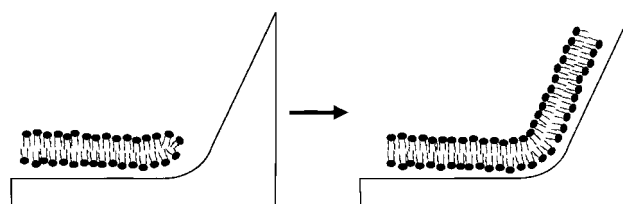


**Figure 9.** A schematic representation of a lipid bilayer spreading at a high curved region of the surface. The bilayer must bend in order to spread.

(Figure 8). This means that in order for the bilayer to expand the surface area per lipid molecule has to increase, a process that becomes increasingly energetically costly as the bilayer continues to stretch out. Finally the bilayer is arrested at the point where the attractive van der Waals interactions between the surface and the bilayer just balance the energy required for bilayer expansion.

Bilayer spreading on mechanically scratched regions of the surface is much less favorable than on smoother portions as demonstrated in Figures 5 and 6. The spreading process over scored regions only became favorable at pH 6 and looked qualitatively different than spreading on smoother surfaces as the bilayer material spread on scratched surfaces along the direction in which the surface was mechanically altered (Figure 3). This suggests that the topography of the underlying surface directly influences the spreading process. Indeed, AFM images of mechanically modified surfaces show that the topography of the surface forms a rake-like pattern of parallel grooves (Figure 7). The glass surface is highly curved between each of these grooves; therefore, it is easy for the bilayer to spread along the direction of a single groove. To propagate from one groove to another while maintaining the favorable van der Waals interactions, the membrane needs to curve around highly contoured regions without increasing the membrane's distance from the surface (Figure 9). To accomplish this, a positive tension needs to be applied to the lower leaflet of the bilayer while a negative tension is applied to the upper leaflet. The

bending energy,  $E_{\text{bend}}$ , associated with this phenomenon is given by<sup>29</sup>

$$E_{\text{bend}} = \frac{1}{2} K_b (1/R_1 + 1/R_2)^2 dA$$

where  $K_b$ , the bending elastic modulus, is multiplied by the integral over the curved area,  $A$ , and  $R_1$  and  $R_2$  are the radii of curvature measured along two perpendicular directions. In the present case we assume that the bilayer is only curving along one direction as the scratch marks used in these experiments were essentially linear, so  $R_2 = \infty$ . For phosphatidylcholine membranes the value of  $K_b$  is approximately  $1.2 \times 10^{-19}$  J.<sup>29</sup> Atomic force micrographs of the scratched glass surfaces cannot be used directly to obtain information on the radius of curvature, because the images do not afford atomic resolution. However, even assuming a radius of curvature for the support of  $R_1 = 30$  nm (a high curvature given the 0.18 rise/run ratios obtained by AFM) and assuming that the bilayer must rigorously follow this radius of curvature, a bending energy of only  $67 \mu\text{J}/\text{m}^2$  is obtained. By comparison the van der Waals attraction is several hundred microjoules per square meter. This suggests that the bending energies of egg phosphatidylcholine bilayers alone are not large enough to make the spreading process on scratched glass unfavorable. Indeed, at low pH, membrane material spreads out over scratch marks quite readily.

The bending elastic modulus depends on the exact chemical content of the lipid bilayer.<sup>29</sup> Because  $E_{\text{bend}}$  is proportional to  $K_b$ , it is expected that altering the chemical composition of the membrane will have a large effect on membrane spreading over roughened surfaces. For example, adding cholesterol to the membrane causes it to stiffen (raising  $K_b$  by a factor of 4), while adding surfactant causes the membrane to become more flexible (lowering  $K_b$  by over an order of magnitude). We have examined membrane spreading around scratched regions for a few altered membrane compositions and found that spreading is unfavorable even at pH 4.5 when cholesterol was added to the membrane. This was presumably the case because the energy per unit area for bending became equal to or greater than the van der Waals interactions. By contrast, adding phosphatidylserine to the membrane (which has fewer waters of hydration associated with each headgroup than phosphatidylcholine) facilitated the spreading process. In this case spreading occurred up to pH 9. We therefore conclude that both surface topographical and hydration properties of the underlying support may govern the prevention of membrane spreading over glass surfaces.

**Consequences for Surface Patterning.** Scratch marks can be used as a simple and flexible method for imposing patterns on supported lipid bilayers creating fluid membrane patches that can be divided from one another for a wide variety of purposes. Surface etching can be performed either before or after deposition of the bilayer and can be used in combination with two-dimensional electrophoresis to create gradients of charged membrane components.<sup>18,21</sup> These scratches can be used in combination with more permanent barriers to lateral mobility created by photo- or electron beam lithography. In this way it

is possible to create and/or heal partitions between regions within permanent boundaries using the results described in this paper, and this can be used to study effects of variable composition and 2-dimensional mixing.<sup>30</sup> Finally, these results suggest the possibility of creating precision features such as mechanical scratches by etching the surface using reactive ion etching (van Oudenaarden and Boxer, to be published).

**Acknowledgment.** The authors thank Prof. Curt Frank and Dr. Christoph Naumann for assistance with the AFM measurements. P.S.C. was supported by an American Chemical Society Irving S. Sigal Postdoctoral Fellowship. This work was supported in part by the CPIMA MRSEC Program of the National Science Foundation under award number DMR-9808677.

## References and Notes

- (1) Tamm, L. K.; McConnell, H. M. *Biophys. J.* **1985**, *47*, 105–113.
- (2) Sackmann, E. *Science* **1996**, *271*, 43–48.
- (3) Tampe, R.; Dietrich, C.; Gritsch, S.; Elender, G.; Schmitt, L. *Nanofabrication and Biosystems: Integrating Materials Science, Engineering, and Biology*; Cambridge University Press: New York, 1996.
- (4) Bayerl, T. M.; Bloom, M. *Biophys. J.* **1990**, *58*, 357–362.
- (5) Johnson, S. J.; Bayerl, T. M.; McDermott, D. C.; Adam, G. W. *Biophys. J.* **1991**, *59*, 289–294.
- (6) Koenig, B. W.; Orts, W. J.; Majkrzak, C. F. *Langmuir* **1996**, *12*, 1343–1350.
- (7) Mou, J. X.; Shao, Z. F. *Biochemistry* **1994**, *33*, 4439–4443.
- (8) Israelachvili, J. *Intermolecular & Surface Forces*, 2nd ed.; Academic Press: London, 1992.
- (9) Keller, C. A.; Kasemo, B. *Biophys. J.* **1998**, *75*, 1397–1402.
- (10) Raedler, J.; Strey, H.; Sackmann, E. *Langmuir* **1995**, *11*, 4539–4548.
- (11) Nissen, J.; Gritsch, S.; Wiegand, G.; Raedler, J. Submitted for publication.
- (12) Vigil, G.; Xu, Z.; Steinberg, S.; Israelachvili, J. *J. Colloid and Interface Science* **1994**, *165*, 367–385.
- (13) Parsegian, V. A. *Langmuir* **1993**, *9*, 3625–3628.
- (14) Parker, J. L.; Rutland, M. W. *Langmuir* **1993**, *9*, 1965–1967.
- (15) Chavez, P.; Ducker, W.; Israelachvili, J.; Maxwell, K. *Langmuir* **1996**, *12*, 4111–4115.
- (16) Hartley, P.; Larson, I.; Scales, P. *Langmuir* **1997**, *13*, 2207–2214.
- (17) Salafsky, J.; Groves, J. T.; Boxer, S. G. *Biochemistry* **1996**, *35*, 14773–14781.
- (18) Groves, J. T.; Boxer, S. G. *Biophys. J.* **1995**, *69*, 1972–1975.
- (19) Groves, J. T.; Boxer, S. G.; McConnell, H. M. *Proc. Natl. Acad. Sci. U.S.A.* **1997**, *94*, 13390–13395.
- (20) Groves, J. T.; Boxer, S. G.; McConnell, H. M. *Proc. Natl. Acad. Sci. U.S.A.* **1998**, *95*, 935–938.
- (21) Groves, J. T.; Wuelfing, C.; Boxer, S. G. *Biophys. J.* **1996**, *71*, 2716–2723.
- (22) Brian, A.; McConnell, H. M. *Proc. Natl. Acad. Sci. U.S.A.* **1984**, *81*, 6159.
- (23) Barenholz, Y.; Gibbes, D.; Litman, B.; Goll, J.; Thomson, T.; Carlson, F. *Biochemistry* **1977**, *16*, 2806.
- (24) Ong, S.; Zhao, X.; Eisenthal, K. B. *Chem. Phys. Lett.* **1992**, *191*, 327–335.
- (25) Wang, D. S.; Pantano, C. G. *J. Non-Crystalline Solids* **1992**, *147&148*, 115–122.
- (26) Israelachvili, J.; Wennerstroem, H. *Nature* **1996**, *379*, 219–225.
- (27) Khachatourian, A. V. M.; Wistrom, A. O. *J. Phys. Chem. B* **1998**, *102*, 2483–2493.
- (28) Du, Q.; Freysz, E.; Shen, Y. R. *Phys. Rev. Lett.* **1994**, *72*, 238–241.
- (29) Sackmann, E. *FEBS Lett.* **1994**, *346*, 3–16.
- (30) Cremer, P. S.; Groves, J. T.; Kung, L. A.; Boxer, S. G. *Langmuir* In press.